

Experimental Observation of High-rate Buckling of Thin Cylindrical Shape-memory Shells

Sia Nemat-Nasser*, Jeom Yong Choi, Jon B. Isaacs, and David W. Lischer
University of California, San Diego, Center of Excellence for Advanced Materials
9500 Gilman Drive, La Jolla, CA 92093-0416
Tel: 858 534-4914; Fax: 858 534-2727; e-mail:sia@ucsd.edu

Abstract

We investigate the buckling behavior of thin cylindrical shape-memory shells at room temperature, using a modified split Hopkinson bar and an Instron hydraulic testing machine. The quasi-static buckling response is directly observed using a digital camera with a close-up lens and two back mirrors. A high-speed Imacon 200 framing camera is used to record the dynamic buckling modes. The shape-memory shells with an austenite-finish temperature less than the room temperature, buckle gradually and gracefully in quasi-static loading, and fully recover upon unloading, showing a *superelastic property*, whereas when suitably annealed, the shells do not recover spontaneously upon unloading, but they do so once heated, showing a *shape-memory effect*. The gradual and graceful buckling of the shape-memory shells is associated with the stress-induced martensite formation and seems to have a profound effect on the unstable deformations of thin structures made from shape-memory alloys.

Keywords: shape-memory alloy, superelasticity, buckling, stress-induced martensite, split Hopkinson bar

1. Introduction

Shape-memory alloys can sustain large strains, up to 6 to 8%, and fully recover without residual deformations. This is called *superelasticity*. While the deformation is fully recovered, the process is dissipative, and the area within the closed loop of the material's stress-strain relation represents the energy lost to heating per unit volume of the sample. In addition, these alloys can display the so-called *shape-memory effect*. In this case, unloading leaves the material in its martensite phase, with a residual deformation that may be recovered upon heating. These

and related unique properties of shape-memory alloys have been studied in connection of variety of potential applications [1-4].

Recently, shape-memory alloys have been considered for potential application in developing multifunctional structures with superior load-bearing/energy absorption, and morphing capabilities [5-7], as well as actively controlling the buckling of the resulting flexible structures [8]. The buckling behavior of tubular structures made of various conventional materials has been studied under both quasi-static and dynamic loading conditions [9-14]. It is reported that the energy absorption capability of the NiTi plates under quasi-static compression loading is superior to that of aluminum plates [15]. However, we are not aware of any study that addresses the direct observation of the buckling behavior of thin shape-memory alloy shells under quasi-static and dynamic loading conditions. For this class of materials, the buckling modes are critically affected by the concomitant austenite to martensite and reverse phase transformations which can prolong the process, dissipate energy, and, because of the superelastic and shape-memory effects, can allow for a full recovery after unloading. Here, we report direct experimental observations of the buckling modes of thin shells made of shape-memory materials, under both quasi-static and dynamic loads, with full recovery due to both superelastic and shape-memory effects.

2. Experimental procedures

The material used in the thin-tube experiments is a shape-memory alloy of composition 55.85wt%Ni-Ti. The thin tubes have 4.5mm outer diameter, 0.125mm wall thickness, and various lengths. In the as-received state, the material's austenite-finish temperature, A_f is 281K. To obtain an alloy with an A_f temperature above 295K, some of the samples are annealed at 773K for 150min.

Quasi-static compression tests are performed using an Instron hydraulic testing machine with a specially designed arbor. The photograph in Figure 1 shows the buckling-test set up for a tube both of whose ends are constrained in maraging steel grips. The tests are conducted at room temperature under a displacement-controlled condition, with crosshead speed of about 10^{-3} mm/s. The axial specimen displacement is measured by a clip gauge, calibrated before testing.

Photographs, synchronized with the corresponding axial load, are taken by a digital camera with a close-up lens.

Dynamic compression tests are performed at room temperature, using a modified split Hopkinson bar system [16,17]. A high-speed Imacon 200 framing camera is used to capture the dynamic buckling behavior of the tubes. Figure 2 is a schematic diagram of the dynamic buckling-test set up. The Imacon 200 framing camera, manufactured by Hadland Inc., can be programmed to record a sequence of separate images. The time delay of each individual channel can be controlled to acquire sixteen images at prescribed time intervals.

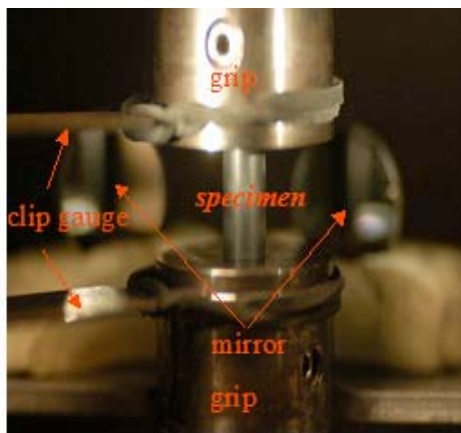


Figure 1 Photograph of the fixed-end buckling-test set up, showing the sample and its reflections in the back mirrors

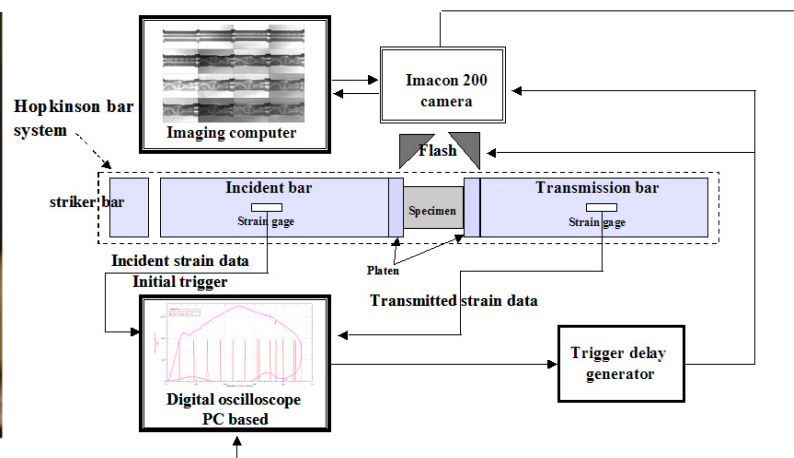


Figure 2 Schematic diagram of the dynamic-test set up, showing the Hopkinson bar, a P.C.-based digital oscilloscope, a trigger delay generator, an Imacon 200 framing camera, and an image processing computer displaying a set of actual images

3. Experimental results and discussion

Buckling under quasi-static loading condition

Figure 3 displays the variation of the load with the displacement under a displacement-controlled loading. Both ends of the tube are fixed, using special grips. The load-displacement curve forms a hysteresis loop, typical of the superelastic loop of shape-memory alloys [18,19]. Figure 4 shows the progressive development of buckling of the shape-memory alloy shell. These pictures are taken directly from the sample at the load levels marked by the corresponding numbers in Figure 3. The buckling begins close to the peak load level (2), after which the load continuously

decreases from (2) to (4). At the maximum displacement of state (4), the sample has buckled into a chessboard pattern. As the displacement is decreased from (4) to (6) in Figure 3, the buckled folds slowly disappear, as shown in Figure 4, with a complete recovery at stage (6). The buckling process in Figure 4 relates directly to the material's phase transformation. During the loading within the superelastic range, the austenitic NiTi transforms into martensites when the buckling begins. As the deformation is continued, transformation from austenite to stress-induced martensite continues, resulting in a gradual and the graceful buckling response of the shell. Upon unloading, a reverse phase transformation, from martensite to austenite, takes place, leading to a full recovery.

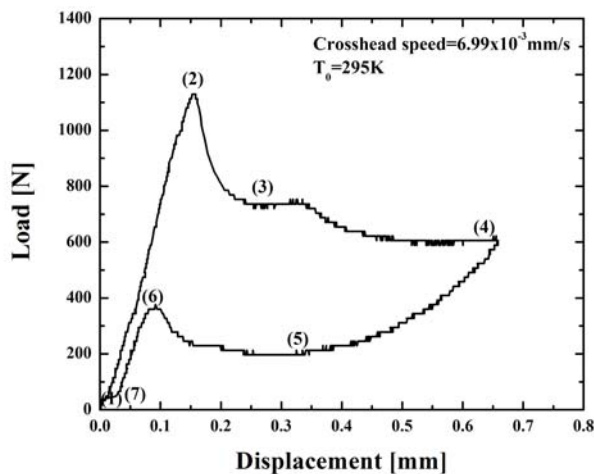


Figure 3 The load-displacement relation for the NiTi tube shown in Figure 4, obtained under a displacement-controlled loading with a crosshead speed of 6.99×10^{-3} mm/s

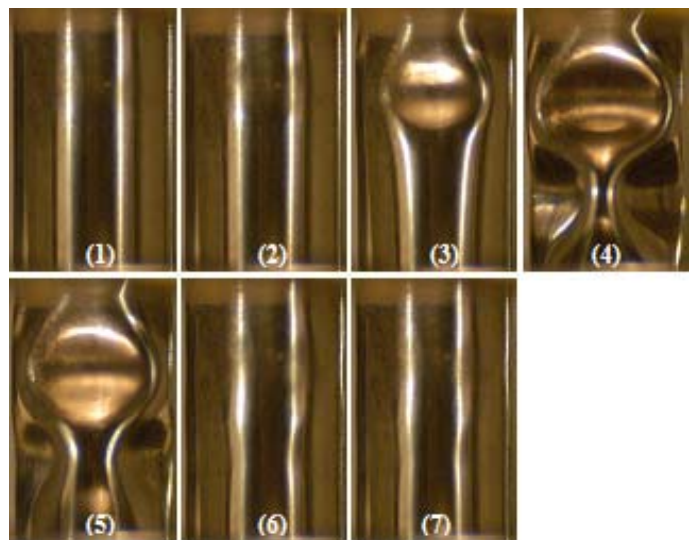


Figure 4 Photographs of NiTi tube buckling ($L/D=1.5$) in uniaxial compression under a displacement-controlled loading with a crosshead speed of 6.99×10^{-3} mm/s; numbers correspond to the load-displacement states of Figure 3

We have also tested some samples with the unconstrained boundary condition. Figure 5 shows the load-displacement curve obtained in this manner for a shell of 1.95 L/D that has been annealed at 773K for 150min. The unloading now leaves a residual displacement, and, unlike in the superelastic case of Figure 3, the hysteresis loop is no longer closed. Upon heating however, the residual deformation disappears and the shell recovers its initial configuration. Figure 6 shows the corresponding buckling modes. The buckling mode is not quite similar to that in Figure 4. As seen in Figure 6, several rings are first formed along the length of the shell during

the loading stages (2) to (4), and then this axially symmetric buckling mode changes to a non-symmetric mode similar to that in Figure 4, leading to a chessboard pattern. The initial ring buckling is not observed in shells of smaller L/D's. The sample in stage (8) in Figure 6 has not recovered, however, but, as shown in Figure 7, it fully recovers upon heating, displaying a typical *shape-memory effect*.

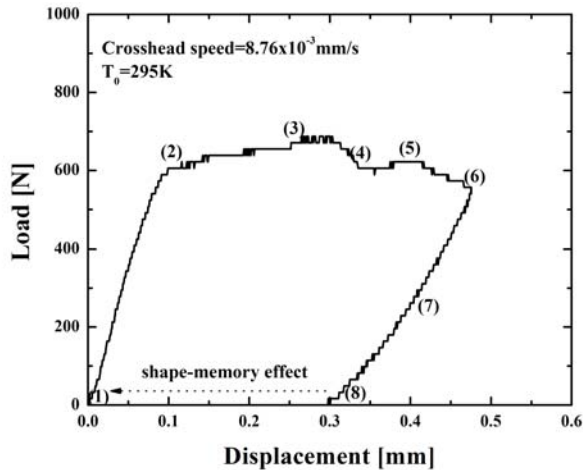


Figure 5 Variation of load with displacement for a NiTi tube with unconstrained ends, obtained under a displacement-controlled loading with a crosshead speed of 8.76×10^{-3} mm/s; the tube is annealed at 773K for 150min, resulting in an A_f temperature higher than 295K

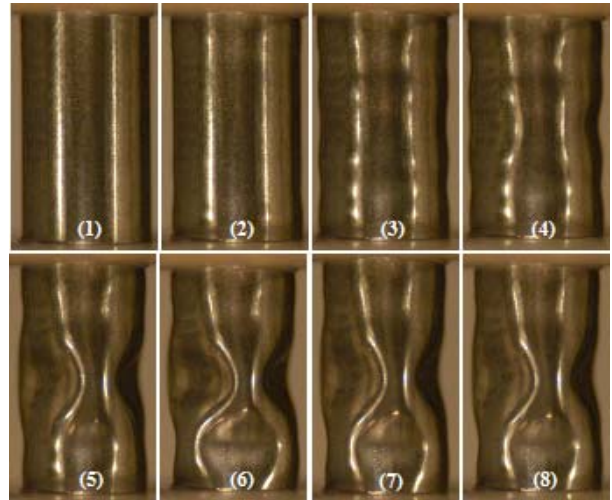


Figure 6 Photographs of NiTi tube with unconstrained ends, buckling in uniaxial compression under a displacement-controlled loading with a crosshead speed of 8.76×10^{-3} mm/s; numbers correspond to the load stages in Figure 5, and the tube is annealed at 773K for 150min, resulting in an A_f temperature higher than 295K

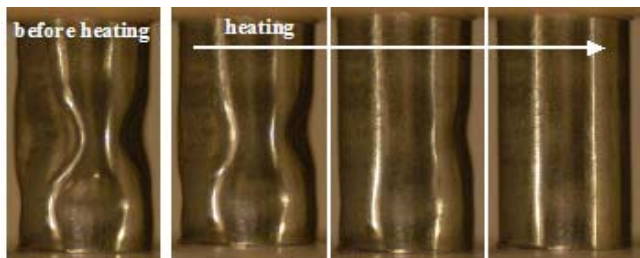


Figure 7 Photographs of the recovery by heating of the buckled NiTi tube, showing a shape-memory effect

Buckling under dynamic loading condition

Using the set up shown in Figure 2, dynamic buckling tests are performed on NiTi cylindrical shells, at a 295K temperature which exceeds the material's A_f temperature of 281K. Below, we use the term "stress" to refer to the axial load divided by the cross-sectional area of the shell, and the term "nominal strain" or simply "strain" to refer to the

total axial shortening of the shell normalized by its initial length; since the sample buckles, both the strain and stress fields are non-uniform throughout the sample. In Figure 8, the periodic spikes denote the camera-timing when the corresponding photo was taken (5 μ sec intervals). The stress-nominal strain curve is also shown in this figure. The sample is a thin NiTi shell of 11.3mm gauge length, 4.5mm outer diameter, and 0.125mm wall thickness. The average nominal strain rate was 1,300/s. As shown in Figure 8, the stress is almost constant until the nominal strain reaches approximately 3.6%, after which, it rapidly decreases as the shell buckles.

The photos, taken at 5 μ sec intervals, are shown in Figure 9. We also note the stress and strain at each picture. At 1.9% strain, the buckling begins by the formation of rings, becoming more pronounced at 2.5 and 3.1% nominal strains, while the stress remains essentially constant. At a nominal strain greater than 3.6%, the rings begin to transform into a chessboard pattern, causing a rapid decrease in the axial load. This chessboard buckling pattern is similar to that observed in the quasi-static case; see Figures 4 and 6.

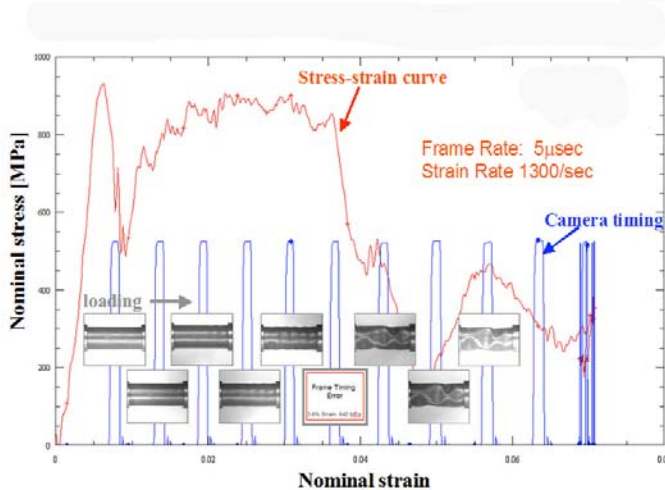


Figure 8 Variation of stress with nominal strain, obtained using mini-Hopkinson bar; L/D is 2.5

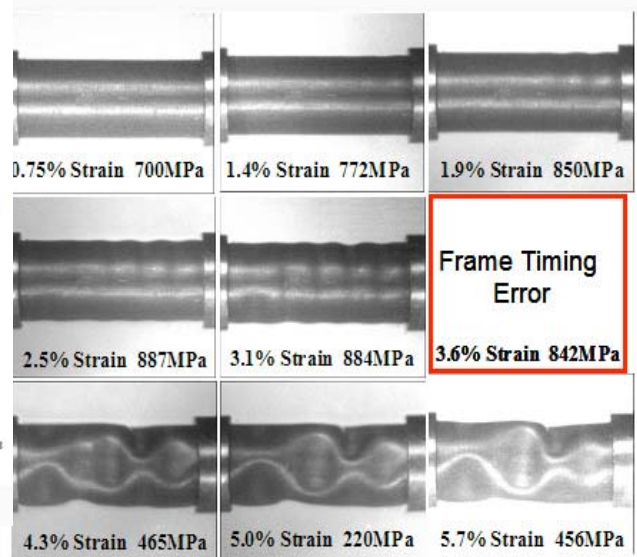


Figure 9 Photographs of the dynamic buckling of a thin NiTi tube, obtained using mini-Hopkinson bar; L/D is 2.5, and the term "strain" refers to the axial shortening divided by L

4. Conclusions

It is observed that the NiTi shape-memory shells with A_f temperature (281K) less than the test temperature (295K), buckle gradually and gracefully, fully recovering upon unloading,

due to their *superelastic property*, whereas the NiTi shells that are annealed at 773K for 150min and have an A_f temperature greater than 295K, do not recover spontaneously upon unloading, but do so once heated, due to their *shape-memory effect*. The initial buckling mode of thin shells depends on their L/D ratio. A thin shell of 1.5 L/D buckles in quasi-static loading into a chessboard pattern, but a thin shell with L/D of 1.95 first forms rings which then transform into a chessboard pattern. A similar buckling mode is observed for a thin shell of 2.5 L/D, deformed dynamically. The stress-induced martensite formation in NiTi shape-memory shells appears to have a profound effect on the shells' unstable deformation, and this can be effectively used to mitigate potential catastrophic failure, dissipate considerably greater amount of energy, and, most importantly, obtain remarkable recovery of the buckled structure.

Acknowledgements: This work was supported by ONR (MURI) grant N000140210666 to the University of California, San Diego.

5. References

- [1] Duerig, T. W., Pelton, A., and Stockel, D., 1999, "An overview of nitinol medical applications," *Mater. Sci. Eng.*, **A237-275**, pp. 149-160.
- [2] Van Humbeeck, J., 2001, "Shape memory alloys: a material and a technology," *Adv. Eng. Mater.*, **3**, pp. 143-156.
- [3] Otsuka, K., and Kakeshida, T., 2002, "Science and technology of shape-memory alloys: new developments," *MRS Bulletin*, Feb, pp. 91-100.
- [4] Saadat, S., Salichs, J., Noori, M., Davood, H., Bar-on, I., Suzuki, Y., and Masuda, A., 2002, "An overview of vibration and seismic applications of NiTi shape memory alloy," *Smart Mater. Struct.*, **11**, pp. 218-229.
- [5] Lu, T. J., Hutchinson, J. W., and Evans, A. G., 2001, "Optimal design of a flexural actuator," *J. Mech. Phys. Solids*, **49**, pp. 2071-2093.
- [6] McGowan, A.-M. R., Washburn, A. E., Horta, L. G., and Bryant, R. G., 2002, "Recent results from NASA's morphing project," *Smart structures and materials: Industrial and commercial applications of smart structures technologies*, SPIE-Vol. 4698, pp. 97-111.

- [7] Elzey, D. M., Sofla, A. Y. N., and Wadley, H. N. G., 2002, "Shape-memory-based multifunctional structural actuator panels," *Smart structures and materials: Industrial and commercial applications of smart structures technologies*, SPIE-Vol. 4698, pp. 192-200.
- [8] Thompson, S. P., and Loughlan, J., 2000, "The control of the post-buckling response in thin composite plates using smart technology," *Thin-walled Struct.*, **36**, pp. 231-263.
- [9] Abramowicz, W., and Jones, N., 1984, "Dynamic axial crushing of circular tubes," *Inter. J. Impact Eng.*, **2**, pp. 263-281.
- [10] Jones, N., 1989, *Structural impact*, Cambridge University Press, Cambridge, UK.
- [11] Reid, S. R., 1993, "Plastic deformation mechanisms in axially compressed metal tubes used as impact energy absorbers," *Inter. J. Mech. Sci.*, **35**, pp. 1035-1052.
- [12] Singer, J., Arbocz, J., and Weller, T., 1998, *Buckling experiments: experimental methods in buckling of thin-walled structures*, John Wiley and Sons Inc, New York, USA.
- [13] Seitzberger, M., Rammerstorfer, F. G., Gradinger, R., Degischer, H. P., Blaimschein, M., and Walch, C., 2000, "Experimental studies on the quasi-static axial crushing of steel columns filled with aluminum foam," *Inter. J. Solids Struct.*, **37**, pp. 4125-4147.
- [14] Alghamdi, A. A. A., 2001, "Collapsible impact energy absorbers: an overview," *Thin-walled Struct.*, **39**, pp. 189-213.
- [15] Suzuki, S., Urushiyama, Y., and Taya, M., 2004, "Energy absorption material using buckling strength of shape memory alloy plate," *Smart structures and materials: active materials: behavior and mechanics*, SPIE-Vol. 5387, pp. 218-226.
- [16] Nemat-Nasser, S., Isaacs, J. B., and Starrett, J. E., 1991, "Hopkinson techniques for dynamic recovery experiments," *Proc. Roy. Soc. Lond.*, **435A**, pp. 371-391.
- [17] Nemat-Nasser, S., and Isaacs, J. B., 1997, "Direct measurement of isothermal flow stress of metals at elevated temperatures and high strain rates with application to Ta and Ta-W alloys," *Acta Mater.*, **45**, pp. 907-919.
- [18] Miyazaki, S., and Otsuka, K., 1989, "Development of shape memory alloys," *ISIJ Inter.*, **29**, pp. 353-377.
- [19] Otsuka, K., and Wayman, C. M., 1998, *Shape memory materials*, Cambridge University Press, Cambridge, UK.